Capturing coronavirus: Comparison and optimization of methods for recovery of infectious coronavirus from environmental surfaces

by

Theresa A. Quintana

B.S., Kansas State University, 2021

A THESIS

submitted in partial fulfillment of the requirements for the degree

MASTER OF PUBLIC HEALTH

Department of Diagnostic Medicine/Pathobiology
College of Veterinary Medicine

KANSAS STATE UNIVERSITY
Manhattan, Kansas

2024

Approved by:

Co-Major Professor
A. Sally Davis

Approved by:

Co-Major Professor
Ellyn Mulcahy

Copyright

Abstract

The unprecedented global impact of the COVID-19 pandemic posed unparalleled challenges to modern-day public health, necessitating the development of effective prevention and control measures across various settings. A critical need has been the development of rigorous and reliable environmental monitoring (EM) strategies to help understand and mitigate viral transmission, especially in crowded working conditions. COVID-19 outbreaks disproportionately affected meat and poultry (M&P) processing facilities early in the pandemic, endangering human and animal health and disrupting the food supply chain. Moreover, an increased reliance on viral RNA detection as a proxy for infectious virus particles has potentially led to inaccurate assessments of the risk of SARS-CoV-2 infection in these environments. Therefore, I evaluated commonly used EM sampling materials and innovative alternatives to identify the most effective material for recovering infectious SARS-CoV-2 particles from non-uniformly inoculated, stainless-steel surfaces, similar to those found in these facilities. Utilizing a systematic approach, I compared the performance of cellulose acetate, hydrophilic polyurethane, and a novel hydrophobic polymer material (MANO) sponge across different sampling sizes and with a variety of eluants.

I found significant variations in different materials' efficacy to recover or release SARS-CoV-2 particles. Polyurethane consistently outperformed the other materials, particularly when compared to MANOs. Specifically, surface sampling with polyurethane at 929 cm^2 and 1,858 cm^2 using a pH 7 beef extract buffer (BEB) solution yielded significantly superior recovery of infectious virus particles compared to MANO recovery from similar surface areas, supporting polyurethane's potential as a preferred material for SARS-CoV-2 EM in M&P environments. Conversely, no statistically significant differences were observed in the comparisons between

cellulose and polyurethane at various sizes, as well as between cellulose and MANO at certain sizes, highlighting the complexity of material performance and the need for nuanced, application-specific considerations.

This research provides empirical evidence to guide the selection of EM materials for infectious SARS-CoV-2 recovery, thereby enhancing the efficiency and reliability of viral detection and surface decontamination strategies. By aligning these insights with the overarching goal of developing, validating, and delivering science-based cleaning and disinfection solutions, this thesis contributes to the broader public health effort to safeguard workers in M&P settings from SARS-CoV-2 exposure.

Table of Contents

List of Figures

List of Tables

Acknowledgments

I wish to express my deepest gratitude to the Master of Public Health program for providing an enriching environment that has fostered my growth and development in this discipline. Furthermore, I am immensely thankful to my committee, whose unwavering guidance, insightful feedback, and continual support have been instrumental in shaping my academic journey. Lastly, a special thanks to my spouse Aaron, whose love, encouragement, and sacrifices have been my bedrock. Your belief in me has been a constant source of strength, making this achievement not just mine, but ours.

Dedication

To those who dream against the odds and rise amidst challenges, this work is dedicated. This endeavor is not just a reflection of my aspirations but a tribute to every hand that held mine, every word that encouraged me, and every sacrifice made in silent support. May this be a testament to our collective dreams and shared journey.

Chapter 1 - Introduction

In late 2019, hospitals in Wuhan, China began to see patients presenting with cases of pneumonia of unknown origin [1]. By January of 2020, the causative agent had been identified as a novel, zoonotic coronavirus, severe acute respiratory syndrome coronavirus 2 or SARS-CoV-2. The virus subsequently spread across the globe, resulting in the Coronavirus Disease 2019 (COVID-19) pandemic declaration in March 2020. SARS-CoV-2 exhibited an infectiousness and transmission efficiency surpassing other genetically related zoonotic coronaviruses, SARS-CoV and Middle East Respiratory Syndrome Coronavirus (MERS-CoV), which caused significant outbreaks in 2002-2003 and 2012, respectively [2].

SARS-CoV originated in central China and demonstrated the capacity for human-to-human transmission but was promptly contained, resulting in approximately 8,000 cases and 774 deaths globally [3]. MERS-CoV, originated in the Arabian Peninsula where it was transmitted to humans, likely from a camel reservoir [4, 5]. MERS-CoV has a higher mortality rate but lower transmission efficiency, leading to sporadic cases and outbreaks primarily confined to healthcare settings [6].

In contrast, SARS-CoV-2's extensive asymptomatic spread, varied clinical manifestations, and delayed global response facilitated its widespread dissemination [7, 8]. As of October 30, 2023, there were 771,549,718 confirmed cases of COVID-19, including 6,974,473 deaths, reported to the World Health Organization [9]. The SARS-CoV-2 pandemic underscored the necessity for robust surveillance, rapid diagnostic capabilities, and effective therapeutic interventions. The unprecedented scale of the COVID-19 pandemic necessitated collaborative

global efforts in research, healthcare, and policymaking aimed to mitigate the impact of the virus and thwart future zoonotic spillovers of such magnitude [10].

SARS-CoV-2

SARS-CoV-2 is a member of the order *Nidovirales*, family *Coronaviridae*, and genus *Betacoronavirus*. It is an enveloped virus with a positive-sense, single-stranded RNA genome approximately 30 kb in length. The SARS-CoV-2 virion consists of four structural proteins surrounding the viral genome (**Figure 1.1**). The spike (S) protein extends from the envelope and binds to the Angiotensin-converting enzyme 2 (ACE2) receptor on human cells for viral entry and is made up of two subunits, S1 and S2 [11]. The S1 subunit facilitates receptor binding, and the S2 subunit enables the fusion of the viral envelope with the host cell membrane [11]. The nucleocapsid (N) protein binds to the viral RNA, forming the nucleocapsid, and is involved in viral replication and virion assembly [12]. The envelope (E) protein is a small membrane protein that plays a role in the assembly and release of the virion [13]. The membrane (M) protein is the most abundant protein in the virion and plays a crucial role in shaping the virus envelope [14].

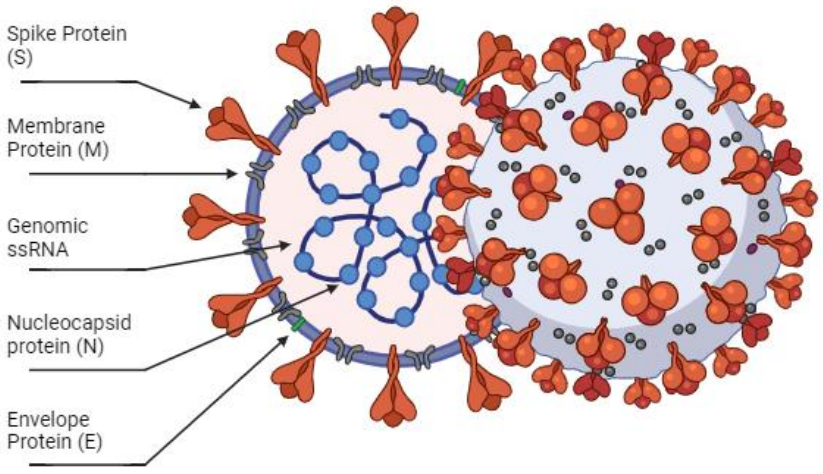

Figure 1.1. SARS-CoV-2 Virion

Illustration of the SARS-CoV-2 virion and important structural proteins. Image created using Biorender.com

Human coronavirus OC43

Human coronavirus OC43 (HCoV-OC43), a member of the genus *Betacoronavirus*, is another coronavirus that can infect humans through the respiratory route. Like SARS-CoV-2, it is also an enveloped virus with a positive-sense, single-stranded RNA genome approximately 30 kb long. However, infection with HCoV-OC43 is primarily associated with mild to moderate respiratory infections and is often the cause of the common cold. The similarities in the two viruses' genetics, transmission, and resistance to disinfection have recommended the use of HCoV-OC43 as a surrogate for SARS-CoV-2 in laboratory experiments [15-17]. Given that SARS-CoV-2 requires higher biosafety levels (BSL-3) due to its heightened pathogenicity and the risk it poses to human health, the ability to use HCoV-OC43 as a surrogate in a less stringent, BSL-2 environment enables researchers to perform critical studies with reduced risk [18]. This has proven especially valuable in the initial stages of research or in facilities where access to higher biosafety levels is limited.

SARS-CoV-2 Transmission

When an infected person coughs, sneezes, talks, or even breathes, they release into the air a range of respiratory and aerosolized droplets containing viral particles. These droplets can be inhaled by individuals in close proximity, typically within about six feet [19]. Airborne transmission in enclosed and poorly ventilated spaces has been a primary concern because in these settings virus-containing aerosols can remain airborne and linger for extended periods of time, increasing exposure time and the potential to infect individuals who share the same environment [20]. Viral particles can also settle on surfaces and objects from the air, leading to the potential for indirect transmission if a person transfers infectious virus on contaminated surfaces to their mucus membranes (face, especially the mouth, nose, or eyes,). Although, indirect transmission from surfaces is now believed to be a less common route of infection [21].

Within meat and poultry (M&P) processing facilities, several constraints make it difficult to control the respiratory transmission of SARS-CoV-2. Due to the nature of their environments, these facilities often have close quarters working conditions, poor ventilation, and additional opportunities for aerosolization (e.g., resuspension during high pressure washing) [22]. Areas with low temperatures and relative humidity extremes are common in M&P processing environments and can further enhance virus stability and persistence on surfaces [23]. Moreover, early in the pandemic, it was not fully understood what risk indirect transmission from contaminated fomites played in virus transmission. Therefore, the concern was that workers could become infected from touching shared equipment and surfaces [24].

SARS-CoV-2 in Meat & Poultry Processing Plants

Among the many sectors affected by the COVID-19 pandemic, the U.S. M&P processing industry faced unique challenges in control and prevention of large-scale outbreaks. Processing

plants are critical components of the food supply chain, producing billions of pounds of meat products annually to meet consumer demand [25]. These processing plants operate on large scales, employing thousands of workers in each facility, making it a significant employer in many regions [26]. The industry involves a range of activities, from slaughtering and butchering to processing and packaging, all of which require close collaboration and coordination among workers. The efficiency and productivity of processing plants are dependent on continuous operations, often in demanding environments with low temperatures and high humidity to maintain product quality and safety. The nature of these facilities, with their high workforce density in prolonged close contact, and often challenging working conditions, makes them highly vulnerable to viral transmission [27].

The significance of understanding the impact of SARS-CoV-2 on M&P processing plants lies in its broader implications for public health and food security. Early in the COVID-19 pandemic there were numerous outbreaks in M&P processing plants, drawing attention to their vulnerability. The rapid spread of the virus within these facilities led to temporary closures, supply chain disruptions, and economic losses. The outbreaks in these facilities not only endangered the health and safety of workers but also disrupted food production and supply, leading to shortages and consumer price increases. Moreover, the virus spread into surrounding communities and caused a public health threat beyond the workplace [28].

Beyond environmental conditions within the M&P plants that facilitate virus transmission, several socioeconomic factors were also important to the spread of COVID-19 among plant workers [29]. These include shared communal settings such as transportation to and from work and multifamily housing. Furthermore, particularly in areas with a significant number of immigrant workers, individuals tended not to immediately seek medical assistance due to fears

about immigration status, lack of access to healthcare, or financial concerns. Additionally, in facilities with a diverse workforce, important information about safety measures and symptoms may not always have been communicated effectively to all workers if not translated into their native languages.

COVID-19 Disease

The SARS-CoV-2 virus can cause asymptomatic to severe COVID-19 disease, influenced by several factors, including the characteristics of the virus itself (agent), the health and pre-existing conditions of the individual (host), and circumstances such as workplace safety, the built environment (man-made infrastructure), socio-economic status, and access to healthcare (environment) as described within the epidemiological triangle (**Figure 1.2**). Mild/moderate disease is characterized by non-life-threatening symptoms and are like those of a common cold or mild flu. These may include fever, cough, sore throat, fatigue, muscle aches, loss of the senses of taste or smell, and gastrointestinal issues such as diarrhea that usually last from a few days to weeks [30]. In contrast, severe disease presents as significant respiratory distress, with symptoms including shortness of breath, chest pain, and confusion. Patients may also experience high fever, a severe cough, and a drop in blood oxygen levels, necessitating supplemental oxygen or mechanical ventilation [31]. Severe COVID-19 can also lead to acute respiratory distress syndrome (ARDS), organ failure, septic shock, blood clots, and multi-organ failure. The risk of death is significantly higher in severe cases, particularly for elderly adults and people with underlying health conditions [32, 33].

A subset of both mild/moderate and severe patients may experience long COVID, also referred to as Post-Acute Sequelae of SARS-CoV-2 infection (PASC) [34]. These patients experience a range of symptoms such as fatigue, shortness of breath, chest pain, joint pain, and

brain fog that continue for weeks or months beyond the initial recovery from the acute phase of COVID-19 disease [35]. Long COVID can significantly impact a person's quality of life, affecting their ability to work, engage in social activities, and perform daily tasks [36, 37]. The persistent nature of symptoms can lead to mental health challenges, including anxiety and depression [38]. The public health impact of long COVID is profound, as the persistent and debilitating symptoms experienced by survivors can lead to a substantial increase in healthcare services use, a decrease in workforce productivity, and a pervasive strain on the individual, their community, and global health resources [39].

M&P workers are particularly vulnerable to infection from SARS-CoV-2 and subsequent development of COVID-19 disease due to a combination of factors inherent to their working and socioeconomic environments [40]. For instance, the physically demanding nature of their job, which involves long hours of standing, repetitive motions, and handling of heavy materials, can lead to chronic physical stress and fatigue. Many workers in this industry come from socioeconomically disadvantaged backgrounds, which may limit their access to healthcare. This lack of access can lead to undiagnosed or poorly managed pre-existing health conditions, such as diabetes or respiratory diseases, which are known risk factors for severe COVID-19 [41]. Moreover, economic pressures, language barriers, and a lack of culturally appropriate health education may lead workers to continue working even when they feel unwell, potentially exacerbating the spread of the virus within the facility.

The initial high rates of infection among workers, coupled with rapidly evolving public health policies, led to staff shortages, reduced operations, and/or temporary shutdowns of M&P facilities [27]. This disruption led to supply chain bottlenecks, affecting the availability of M&P products in the market and subsequent price increases. Disruption within the industry also

created significant animal welfare issues [42]. A backlog of animals ready for slaughter but with nowhere to go led to overcrowding on farms, straining feed supplies and space. Limited processing capacity forced farmers to make difficult decisions, including the culling and disposal of animals that could not be processed in a timely manner [27]. These impacts highlight the interconnected nature of the agriculture industry and public health, underscoring the need for more resilient and adaptable systems.

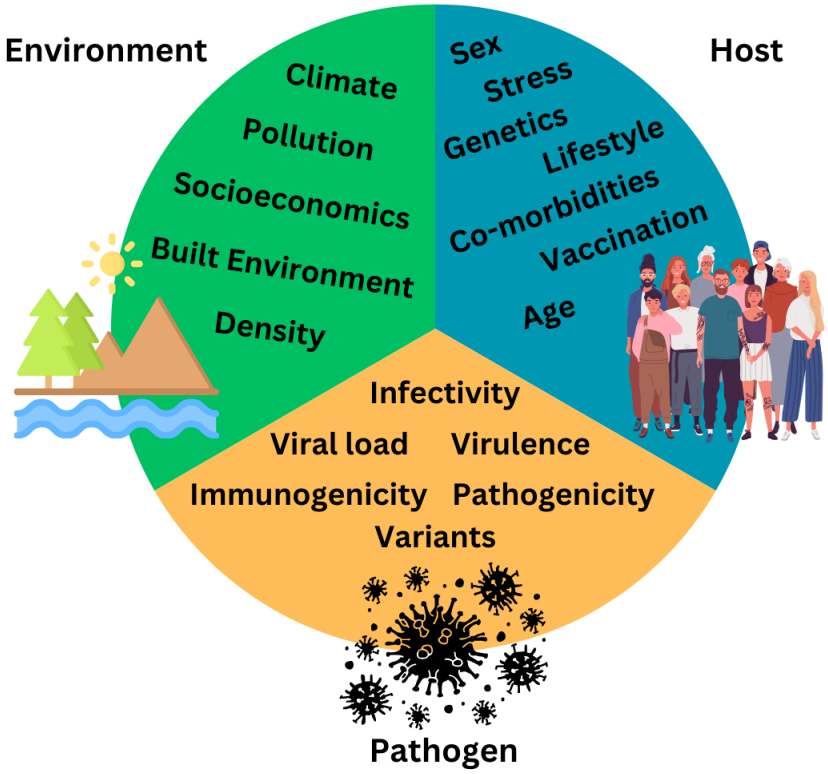

Figure 1.2. Epidemiological triad of factors influencing the development of severe COVID-19

Public Health Prevention Measures

Historical respiratory pandemics, such as the 1918 Influenza Pandemic and the H1N1 Influenza Pandemic in 2009, played a crucial role in shaping the public health measures implemented during the COVID-19 pandemic. During the 1918 influenza outbreak (a.k.a.

"Spanish Flu") non-pharmaceutical interventions like isolation, quarantine, good personal hygiene, use of disinfectants, and limitations on public gatherings were widely applied [43]. Although the scientific understanding and technological capabilities of the time were limited compared to today, these measures still helped to mitigate the spread of the virus and provided early insights into the effectiveness of community-wide public health interventions. Moreover, the H1N1 pandemic in 2009, while less severe, provided valuable lessons in rapid vaccine development, distribution, and the importance of clear, transparent communication from health authorities [44]. These historical experiences underscored the importance of quick action, robust public health infrastructure, and global cooperation, all of which were paramount in the response to the COVID-19 pandemic. They also highlighted the critical need for the swift development of diagnostic tests and vaccines, emphasizing the necessity of ongoing investment in public health preparedness to ensure readiness for future pandemics [45].

In response to the SARS-CoV-2 pandemic, M&P plants implemented a range of mitigation strategies in accordance with federal and local guidelines to prevent the spread of the virus and protect their workforce [46]. These included enhanced hygiene and sanitation protocols, with increased cleaning and disinfection, along with the use of personal protective equipment (PPE) such as masks, face shields, and gloves for all employees [47]. Social distancing measures were introduced, involving the reconfiguration of workstations and the use of physical barriers to ensure appropriate spacing [47]. Health screenings, including temperature checks and regular COVID-19 testing to monitor employee health, became routine. Workforce density was decreased by introducing staggered shifts and break times [46]. Extensive education and training on COVID-19 safety protocols were provided to employees [46]. Supportive measures, such as encouraging workers to stay home when unwell and provision of paid sick

leave, were also adopted. Additionally, vaccination campaigns were encouraged to build employee immunity [48]. In cases of confirmed infections, rapid response protocols, which included isolation and contact tracing, were implemented to prevent further spread. These comprehensive efforts were crucial in safeguarding the health of workers while maintaining the critical food supply chain [47].

However, despite safe and efficacious vaccines and proven preventative measures, the COVID-19 pandemic highlighted political and social issues that impacted the success of public health prevention measures. Inconsistent messaging and lack of coordination from political leaders hindered the uniform implementation of public health measures [49]. Moreover, the politicization of the pandemic and rampant misinformation/propaganda, where preventive measures like mask-wearing and lockdowns became politically charged topics, led to resistance from certain groups and undermined the public's trust in authorities and scientific experts. Bureaucratic hurdles delayed the implementation of public health measures and inequities in policy enforcement and resource allocations resulted in marginalized communities often facing harsh repercussions such as increased morbidity and mortality [50].

The socioeconomic impact of the COVID-19 pandemic response also led to widespread frustration and opposition to public health measures. The economic downturn and job losses due to lockdowns and other restrictions, as well as essential workers - often in lower-paying jobs- facing increased virus exposure risks, highlighted social inequalities [51]. Prolonged isolation, economic uncertainties, and fears of infection contributed to a mental health crisis [52, 53]. Disruptions to education and youth services have led to longer-term implications for learning and development, especially in underprivileged communities [54]. The unequal global distribution of vaccines underscored international disparities and threatened global control of the pandemic

[55]. These sociopolitical issues surrounding COVID-19 public health prevention measures highlight the complexity of managing a global pandemic. Addressing these challenges requires a multifaceted approach, which emphasizes transparent communication, equitable resource distribution, and fostering trust and solidarity at all levels of society.

Knowledge Gap

The critical need for effective public health interventions within M&P environments is apparent in the wake of the SARS-CoV-2 pandemic. However, a noticeable gap in knowledge exists regarding optimal strategies for enveloped virus detection in these facilities. To comply with federal food safety requirements, M&P environmental monitoring (EM) programs already use a variety of samplers (e.g., sponges, swabs, wipes), materials, and eluants for the surveillance of bacterial or non-enveloped food-borne pathogens [56]. However, their efficacy in specifically recovering infectious SARS-CoV-2 from diverse surfaces is not comprehensively understood [57]. Additionally, although measuring viral RNA copies is commonly employed as an indirect indicator of the presence of infectious virus because it is quicker, it is more precise and relevant for risk assessment to directly measure infectious virus levels.

Acknowledging this gap, I conducted a systematic evaluation of commonly used EM materials for sponge samplers, including cellulose acetate and hydrophilic polyurethane, alongside a novel hydrophobic polymer material (Innovaprep MANOs). Additionally, I examined these EM materials with either a beef extract buffer at pH 7, with and without Tween-20, as well as a phosphate buffered saline with Tween-20, to assess the impact of surfactants, buffering capacity, and virus stability on the elution efficiency of these materials. By studying their performance under the manufacturer's suggested optimal and maximum sampling areas, I

sought to uncover the most effective combination for recovering infectious SARS-CoV-2 particles.

Chapter 2 - Capturing coronavirus: Comparison and optimization of recovery methods for infectious coronaviruses from environmental surfaces

1. Introduction

Outbreaks of COVID-19 in United States (U.S.) meat and poultry (M&P) processing plants resulted in 16,233 worker infections, spanning twenty-three states and 239 facilities by May 2020 [58, 59]. The resulting plant closures and reduced production due to worker illnesses, as well as lockdowns and social distancing requirements, caused pervasive disruptions to the U.S. food supply. This led to increased meat prices and losses of five billion and thirteen billion dollars in revenue for the pork and beef industries, respectively [27, 60, 61]. The M&P industry faced unique challenges in the prevention and control of SARS-CoV-2 transmission within their facilities, including high-density employee working conditions with prolonged contact between workers, recirculated or low air exchange rates, and low temperature, high humidity conditions within the plant that are favorable for the SARS-CoV-2 virus stability [22].

The SARS-CoV-2 virus, the etiological agent of COVID-19 disease, belongs to the *Coronaviridae* family and is an enveloped virus with a single-stranded, positive-sense RNA genome [1]. Coronaviruses commonly induce respiratory illnesses in both humans and animals and are primarily spread through the release of virus-containing respiratory droplets and aerosols by an infected individual when they cough, talk, or sneeze [19]. For SARS-CoV-2, prolonged close contact with an infected individual, especially in crowded or poorly ventilated indoor settings, can significantly increase the risk of infection because aerosols containing infectious virus particles can remain suspended in the air for extended periods [62]. Moreover, under

suitable conditions SARS-CoV-2 has been demonstrated to stay infectious on surfaces for several hours to days [63]. Initially, the significance of SARS-CoV-2 transmission via direct contact from virus-contaminated inanimate objects (fomites) was unclear. Our current understanding suggests the role of fomites in the transmission of SAR-CoV-2 is minor; however, uncertainty at the onset of the pandemic led to concerns that the virus could be transmitted from infected workers in M&P processing facilities to food products and then to consumers [21, 64, 65]. Consequently, the need for Environmental Monitoring (EM) for SARS-CoV-2 was considered crucial to understanding virus transmission dynamics within these facilities to aid efforts to implement targeted prevention strategies [24].

Food manufacturing facilities primarily focus their EM programs on detecting bacterial pathogens like *Salmonella* and *Listeria*, and on assessing public health risks by examining animal carcasses and environmental surfaces [66-70]. Comprehensive EM programs enable the prompt identification and recall of potentially contaminated products, reducing foodborne disease outbreaks [56]. These programs typically use advanced detection methods like polymerase chain reaction (PCR) and enzyme-linked immunosorbent assays (ELISA) to quickly and accurately identify the presence of bacterial pathogens. However, the effectiveness of a comprehensive EM program in the identification and quantification of bacterial contamination in these environments hinges on the robustness and precision of the EM tools employed for sampling [71]. While these EM programs are essential for ensuring compliance with FDA and USDA food safety requirements, standardized program requirements do not yet exist. Consequently, the M&P industry has developed and adopted a wide variety of methods, with significant variability between facilities in terms of sampler materials, elution buffers, surface areas sampled, and diagnostic assays [72, 73].

Several viruses, like norovirus, are also food-borne pathogens of concern to public health, and the development of EM techniques designed for non-enveloped viruses has been described [74, 75]. Unlike bacteria, viruses do not adhere to surfaces and may require the use of specialized samplers, eluants, and sampling areas to effectively collect intact virus particles. The optimization of these techniques is essential to ensure accurate and reliable results, as the use of devices and procedures primarily designed for bacteria may not be sufficient or appropriate for studying viral pathogens. For instance, in the surveillance of human norovirus, murine norovirus, and Tulane virus, the composition of the sampler material, elution buffers used, and surfaces tested have all been critical to the efficient recovery of infectious virus from surfaces [57, 76, 77].

Moreover, EM surveillance of viruses has largely been focused on the detection of viral nucleic acids because of the safety, speed, sensitivity, and broad applicability of qPCR and RT-qPCR techniques, making it the preferred method for detecting viruses [78, 79]. Nucleic acid detection is often used as a proxy measurement for viral load despite an inadequate understanding of how the number of viral gene copies relates to infectivity. Since nucleic acids can be extracted from both intact and degraded virions, using nucleic acid detection as a measure for infectivity may not reliably indicate the presence of infectious viruses or the associated risk of transmission [80]. Miyazaki et al demonstrated that nucleic acid recovery of influenza A and feline calicivirus were significantly higher than the recovery of the infectious viruses, highlighting the limitations in accurately assessing the risk of infections using nucleic acid data alone [77]. Therefore, quantification of infectious viruses rather than viral nucleic acid is crucial to provide a more accurate assessment of transmission risk for SARS-CoV-2 in M&P environments. While RNA detection has been used to aid in surveillance efforts of SARS-CoV-

2, to our knowledge, surface sampling techniques and stable eluants for EM in M&P that help maintain SARS-CoV-2 infectivity for virus recovery remain sparse [81, 82]

In this study, I tested several commonly used EM materials (cellulose acetate, hydrophilic polyurethane), a novel hydrophobic polymer material (MANOs), and eluants at the manufacturer's suggested optimal and expanded sampling sizes to identify the best combination for infectious SARS-CoV-2 recovery from directly inoculated stainless steel (SS) surfaces.

2. Materials & Methods

2-1. Cell lines and virus stocks

Human ileocecal colorectal adenocarcinoma cells (HRT-18, CCL-244) and African green monkey kidney epithelial cells (VeroE6, CRL-1586) were purchased from the American Type Culture Collection (ATCC) in Manassas, VA. HRT-18 cells were grown in Roswell Park Memorial Institute 1640 (ATCC formulation; RPMI 1640, Gibco, Fisher Scientific, Palatine, IL) medium supplemented with 10% heat-inactivated fetal bovine serum (HI-FBS, Gibco, Fisher Scientific, Palatine, IL), 1X l-glutamine (Corning, Fisher Scientific, Palatine, IL), and 1X penicillin-streptomycin (Corning, Fisher Scientific, Palatine, IL). VeroE6 cells were grown in Eagle’s Minimum Essential Medium (EMEM, Corning, Fisher Scientific, Palatine, IL) supplemented with 10% HI-FBS, 1X l-glutamine, and 1X penicillin-streptomycin. Both cell lines were grown in a humidified incubator at 37°C with 5% CO_2.

Due to the highly contagious nature of SARS-CoV-2 and its potential for airborne transmission, research on the virus is restricted to biosafety level (BSL)-3 facilities. Consequently, we chose to use a surrogate BSL-2 virus to maximize investigator safety during

development of viable virus recovery methods. We selected human β-coronavirus OC43 (OC43) because of its similar morphology and inactivation profile [17, 83].

OC43 (VR-1558) was acquired from ATCC. OC43 was passaged twice in HRT-18 cells in RPMI 1640 medium supplemented with 2% HI-FBS, 1X L-Glutamine, and 1X penicillin-streptomycin. HRT-18 cells were infected at a multiplicity of infection (MOI) of 0.1 and then incubated in a humidified incubator at 33°C with 5% CO_2 for 4 days. After one freeze/thaw cycle, the cells and supernatant were centrifuged at 500 × g for five minutes at room temperature (RT), and the supernatant was aliquoted and stored at -80°C until titration or use.

All SARS-CoV-2 propagation and experiments were conducted at the Kansas State Biosecurity Research Institute (BRI, Manhattan, KS) in BSL-3 containment. SARS-CoV-2 strain WA1/2020 was acquired from Biodefense and Emerging Infections Research Resources Repository (BEI Resources; Bethesda, MD) and propagated via blind passage three times in VeroE6 cells in EMEM supplemented with 2% HI-FBS, 1X l-glutamine, and 1X penicillin-streptomycin and incubated at 37°C with 5% CO_2 until 80% or more cytopathic effect (CPE) was observed. After one freeze/thaw cycle, the cells and supernatant were centrifuged at 500 × g for five minutes at RT and the supernatant was aliquoted and stored at -80°C until titration or use.

2-2. Virus Titration

Titers of OC43 and SARS-CoV-2 were determined using a tissue culture infectious dose 50% ($TCID_{50}$) assay on HRT-18 and VeroE6 cells, respectively. Briefly, appropriate cells were seeded in 96-well plates and incubated in a humidified incubator at 37°C with 5% CO_2 until 80% confluency was reached. The medium was then removed, and the cells were inoculated with 10-fold dilutions of stock virus or virus samples in duplicate for three biological replicates. Plates

were incubated for three (SARS-CoV-2) or four (OC43) days in a humidified incubator at 37°C or 33°C, respectively, with 5% CO_2. Indirect immunofluorescence was used to detect OC43 as previously described [83]. Briefly, the cells were fixed with 4% paraformaldehyde, labeled with mouse anti-OC43 N protein primary monoclonal antibody (Millepore Sigma, St. Louis, MO) at 1:2000, and donkey anti-mouse Alexa Fluor 488 secondary antibody (Jackson ImmunoResearch, West Grove, PA) at 1:400. SARS-CoV-2 induced CPE was detected by staining with crystal violet fixative (25% of 37% formaldehyde (Fisher Chemical, Fair Lawn, NJ), 10.5% of 95% ethanol (Decon Laboratories, King of Prussia, PA), 5% glacial acetic acid (Fischer Chemical, Fair Lawn, NJ), 59.5% distilled water, and 2 g crystal violet powder (Acros Organics, Geel, Belgium) for one hour. Wells were screened for fluorescence (OC43) using an Olympus CKX53 fluorescence microscope or manually screened (SARS-CoV-2) for CPE. All samples were run in duplicate. Titers were calculated using the Reed and Muench method and averaged [84].

2-3. Sampling tools and eluants

Samplers

Hydrophilic, cellulose acetate sponges (cellulose, Nasco, Fisher Scientific, Palatine, IL, and VWR® Avantor, Radnor, PA), hydrophobic, open-cell, polymeric foam, Mano Surface Samplers (MANOs, InnovaPrep LLC, Drexel, MO), and hydrophilic, polyurethane foam EZ Reach™ sponge samplers (polyurethane, World Bioproducts, Libertyville, IL) were acquired and tested for their recovery of infectious OC43 and/or SARS-CoV-2 (**Figure 2.1**).

Figure 2.1 Samplers

Hydrophilic cellulose acetate (left), hydrophobic, open-cell, polymeric foam, InnovaPrep MANO Surface Sampler (center), and hydrophilic polyurethane foam, EZ Reach™ sponge samplers (right)

Eluants

MANOs came pre-soaked with 20 ml phosphate buffered saline with 0.05% Tween-20 (PBS/T). However, stability studies within our laboratory (unpublished data) identified a beef extract buffer comprised of 100 mM Tris base (Sigma-Aldrich, St. Louis, MO), 50 mM glycine (Thermo Fisher Scientific, Fair Lawn, NJ), 50 mM magnesium chloride (Acros Organics, Geel, Belgium), and 1.5% beef extract (MP Biomedicals, LLC, Solon, OH), with pH adjusted to 7.0 (BEB7), to be a robust stabilizing eluent for OC43 and SARS-CoV-2. InnovaPrep produced a limited number of MANOs custom filled with 20 ml BEB7 and BEB7 with 0.05% Tween-20 (BEB7/T). BEB7 was used with cellulose and polyurethane. BEB7/T was used with cellulose.

Surface Areas

100 cm^2 was determined to be the optimal surface area for cellulose sampling and 300 cm^2 was chosen as an expanded area based on literature regarding bacterial sampling and guidance from food safety and environmental monitoring experts [75]. The surface areas for MANOs were based on guidance from InnovaPrep. According to the manufacturer, the optimal sampling area was 1,267 cm^2; however, a maximum expanded area of 1 m^2 could be used. Within a biological safety cabinet (BSC), we tested surface areas of 1,267 cm^2 and 7,600 cm^2, the maximum area available within the BSC. The surface areas for polyurethane were based on product instructions from World Bioproducts regarding bacterial sampling. In addition to the recommended optimal area of 1,858 cm^2 for polyurethane, more conservative areas of 100 cm^2 and 969 cm^2 were tested for infectious virus recovery.

Therefore, I will refer to 100 cm^2, 1,267 cm^2, and 1,858 cm^2 for cellulose, MANOs, and polyurethane, respectively, as the optimal sizes while 300 cm^2 and 1 m^2 (7,600 cm^2) will be referred to as the expanded sizes for cellulose and MANOs, respectively. Finally, the conservative sizes for polyurethane are 100 cm^2 and 969 cm^2.

All experiments were conducted on SS surfaces. SS was selected due to its prevalence, uniformity, ease of sanitation, and ability to provide consistent, comparable results.

2-4. Experimental Design

OC43 and SARS-CoV-2 BSC Studies

Experimental methods for studies conducted within the BSC for OC43 and SARS-CoV-2 are illustrated in **Figure 2.2**. Dry cellulose sponges were soaked with 15 ml BEB7 or BEB7/T immediately prior to use. MANOs, stored at -20°C, were thawed prior to use. Using stencil

templates and a sharpie, 100 cm^2 and 300 cm^2 (cellulose), or 1,267 cm^2 and 0.76 m^2 (MANOs) areas were drawn onto the SS surface of the BSC. Each device, eluant, and area combination were tested in triplicate. For OC43, ten 10 µl drops of neat virus stock (2.61 $\times 10^6$ $TCID_{50}$/ml) were inoculated onto the marked areas, either 100 cm^2 (cellulose) or 1,267 cm^2 (MANOs), for a total of 100 µl (2.61 $\times 10^5$ $TCID_{50}$). For the larger areas, (300 cm^2 for cellulose and 7,600 cm^2 for MANOs), ten 10 µl drops of diluted virus (1.00 $\times 10^5$ $TCID_{50}$/ml) were inoculated onto the marked areas for a total of 100 µl (1.00 $\times 10^4$ $TCID_{50}$). All areas were immediately sampled using the appropriate sampler according to the manufacturer's instructions (**Figure 2.2**). If only a single marked area fit within the BSC, the BSC surface was decontaminated by wiping with 70% ethanol, Accel Hydrogen Peroxide wipes (Diversey, Fort Mills, SC), and then again with 70% ethanol after sampling. The BSC surface was allowed to dry completely before demarcating a new area.

Cellulose and MANOs were processed for virus recovery by squeezing the sponge and allowing the liquid to be drawn back thrice. The sponges were then wrung of all possible fluid and the remaining eluant was collected with a serological pipette (cellulose) or 20 ml Luer Lock syringe (MANOs), and the volume was recorded, aliquoted, and stored at -80°C until batch titration. Identical experiments were conducted at BSL-3 with SARS-CoV-2 except that only 100 cm^2 (cellulose) and 1,267 cm^2 (MANOs) were tested using 5.01 $\times 10^5$ $TCID_{50}$ of virus. An additional sampling method was performed for cellulose, where the eluant was wrung out prior to wiping the surface, and both sides of the sponge were used in an overlapping pattern, vertically and horizontally, to try to increase virus recovery.

SARS-CoV-2 BSL-3 Agricultural Containment Space

To accurately simulate sampling efforts within M&P manufacturing facilities, where airflow turnover rates are significantly lower than within a BSC, I conducted additional experiments within a BSL-3 Ag containment space where room air exchange rates were reduced to six exchanges per hour. Experiments were conducted identically to those done within the BSC, except BEB7 was the only eluant tested. Lower than expected recovery of OC43 and SARS-CoV-2 in BSC experiments prompted the addition of polyurethane sponges, as they were demonstrated in the literature to be a more efficient EM sampler [74]. Polyurethane sponges were tested for all three surface areas (100 cm^2, 969 cm^2, and 1,858 cm^2) and MANOs were tested at 1 m^2. SARS-CoV-2 stock virus diluted to 5.72×10^5 $TCID_{50}$/ml and 5.72×10^4 $TCID_{50}$ was inoculated onto each surface. Sample collection using polyurethane was performed according to the manufacturer's instructions. Briefly, polyurethane sponges presoaked in 10 ml BEB7 in sealed, sterilized bags were used to collect the virus within the surface area, using only one side of the sponge and wiping along the surface in an overlapping vertical and horizontal pattern (**Figure 2.3**).

Two controls were used to determine the origin of potential recovery losses. The first was direct inoculation of each eluant pre-soaked sponge tool. The second was direct inoculation into the eluant-containing bag for each sponge prior to the addition of the sponge. All the samples were stored at 4°C until processing in a BSL-3 laboratory. All the samples were processed within five hours of collection as previously described and stored at -80ºC until batch titration.

Analysis

All $TCID_{50}$ measurements were performed in duplicate and averaged. The percent recovery was calculated by dividing the mean recovered $TCID_{50}$ for each sample by the applied inoculum $TCID_{50}$ value and multiplying by 100. Comparisons of means for samplers, area size, and controls were analyzed using one-way ANOVA (α=0.05), followed by Šídák's multiple comparisons test in GraphPad Prism9 (www.graphpad.com). Data was graphed using Microsoft Excel or GraphPad Prism9 software.

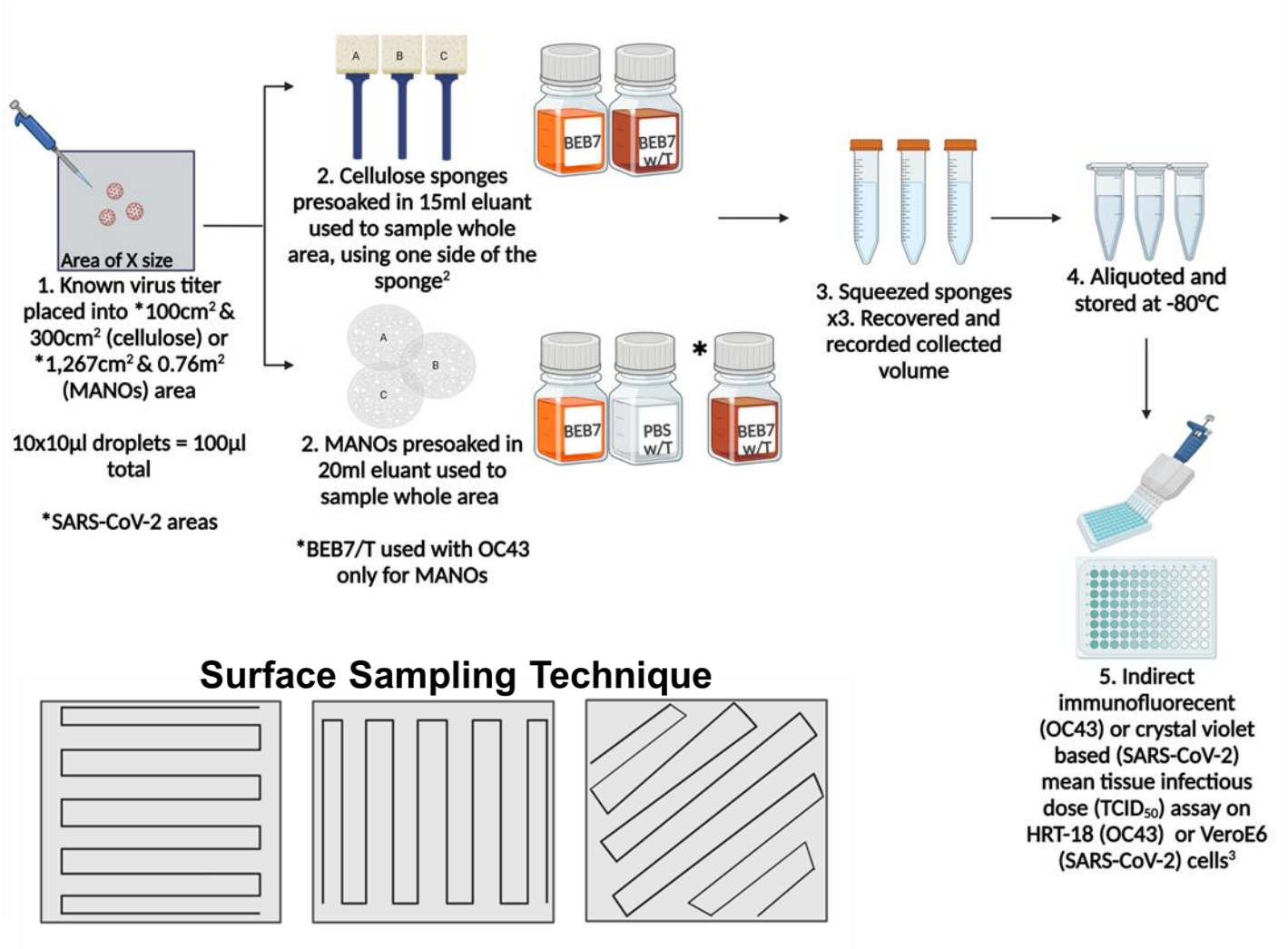

Figure 2.2. Overview of experimental methods for OC43 and SARS-CoV-2 inside a BSC

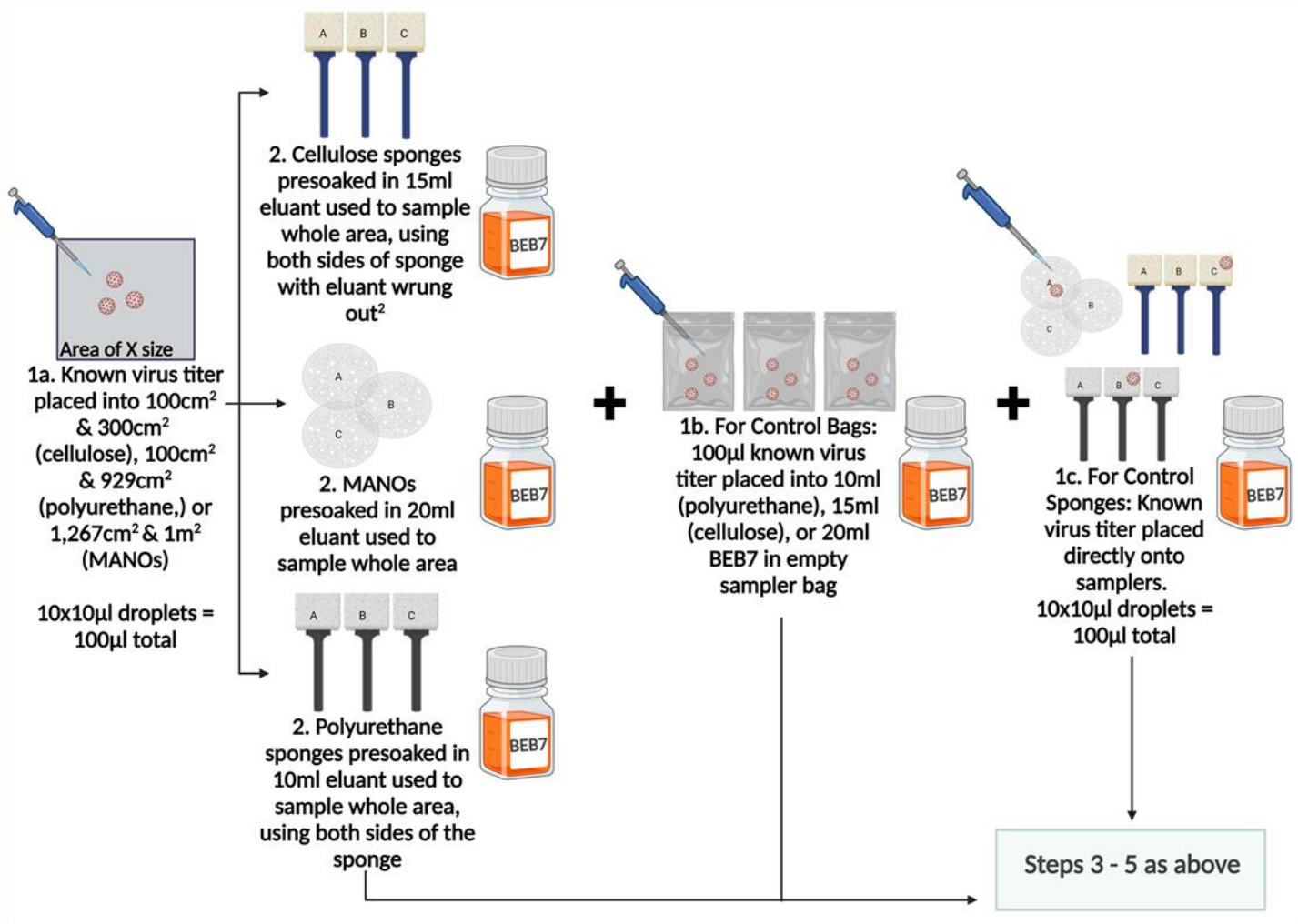

Figure 2.3. Overview of experimental methods for SARS-CoV-2 in BSL-3 Ag containment space.

3. Results

3-1. Infectious OC43 Recovery Comparisons

Different combinations of samplers (cellulose, polyurethane, and MANOs) with eluants (BEB7, BEB7/T, and PBS/T) were evaluated using OC43 prior to working with SARS-CoV-2 at BSL-3. There were no significant differences in the recovery of infectious OC43 between cellulose and MANOs at the optimal surface areas with BEB7 and BEB7/T (**Figure 2.4**). Moreover, comparisons between cellulose and MANOs with BEB7 and BEB7/T at optimal sizes did not exhibit significant differences in percent recovery. However, MANOs with BEB7 and BEB7/T had a 51% - 85% greater average percent recovery than PBS/T at optimal surface areas ($p = 0.0038$ and $p = 0.0275$, respectively) (**Figure 2.4 B**). Moreover, when the surface areas were expanded for both cellulose and MANOs, infectious virus was only recovered using cellulose BEB7/T (32%). During this experiment, I observed significant inefficiencies in the resorption of the eluant when using hydrophobic MANOs

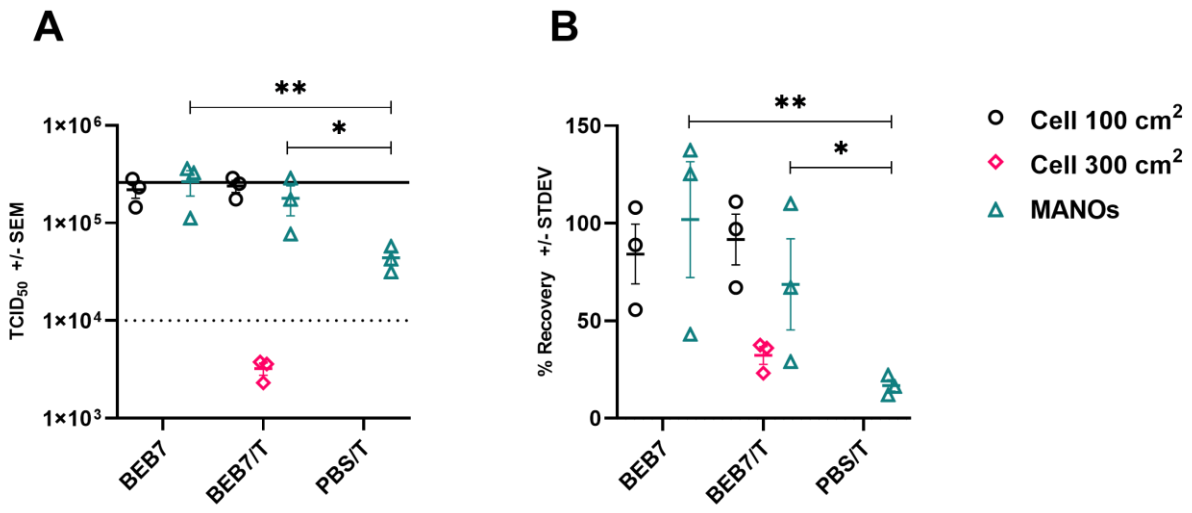

Figure 2.4. OC43 recovery from SS in eluants using samplers.

Total $TCID_{50}$ recovery (A) and percentage of recovery (B). The horizontal solid line denotes the initial inoculum of 2.61 $\times 10^5$ $TCID_{50}$ for MANOs and cellulose (Cell) at optimal sizes. The dashed horizontal line denotes the starting inoculum of 1.00 $\times 10^4$ $TCID_{50}$ for the expanded sizes applicable to Cell 300 cm^2 only. Bars represent the standard error of the mean (SEM; A) and standard deviation (STDEV; B). The symbols *, and ** denote the significance levels of a p-value where *: $p \leq 0.05$, **: $p \leq 0.01$.

3-2. Recovery Comparisons of Infectious SARS-CoV-2 inside a BSC

Based on the recovery results with infectious OC43, subsequent studies were conducted with SARS-CoV-2; however, MANOs with BEB7/T were excluded because for OC43 there were no significant differences in recovery between BEB7 and BEB7/T. Additionally, samplers and eluants were only tested within the optimal sizes due to the general failure to recover infectious OC43 at the expanded areas in the BSC. The percent recovery of infectious SARS-CoV-2 using MANOs with BEB7 was on average 26.6% greater than with PBS/T ($p= 0.0001$) (**Figure 2.5 B**). There was no difference in recovery of infectious SARS-CoV-2 between cellulose and MANOs with BEB7. Also, there was no statistically significant difference in the percent recovery between cellulose with BEB7 and BEB7/T.

Bacteriological EM, cellulose sponges are often wrung out before use, and surfaces are sampled using both sides of the sampler (personal communication with Randall Phebus). Therefore, I compared the recovery of SARS-CoV-2 between wrung-out cellulose using both sides for sampling with my previous sampling method (left soaked, one side used) on a 100 cm^2 area, the optimal size. Subsequently, I observed no significant difference between the two methods (**Figure 2.5**).

Notably, a significant decrease in the recovery of infectious SARS-CoV-2 compared to OC43 was observed for optimal sizes across all samplers and eluants (**Figure 2.6**). The greatest differences in average percent recovery between OC43 and SARS-CoV-2 were seen with MANOs with BEB7 (75% average decrease, $p = 0.0195$) and cellulose with BEB7 (62% average decrease, $p = 0.0459$). Furthermore, there were 74% and 16.5% decreases in the recovery of SARS-CoV-2 compared to OC43 using cellulose with BEB7/T ($p = 0.0062$) and MANOs with PBS/T ($p < 0.0001$) (**Figure 2.3 B**).

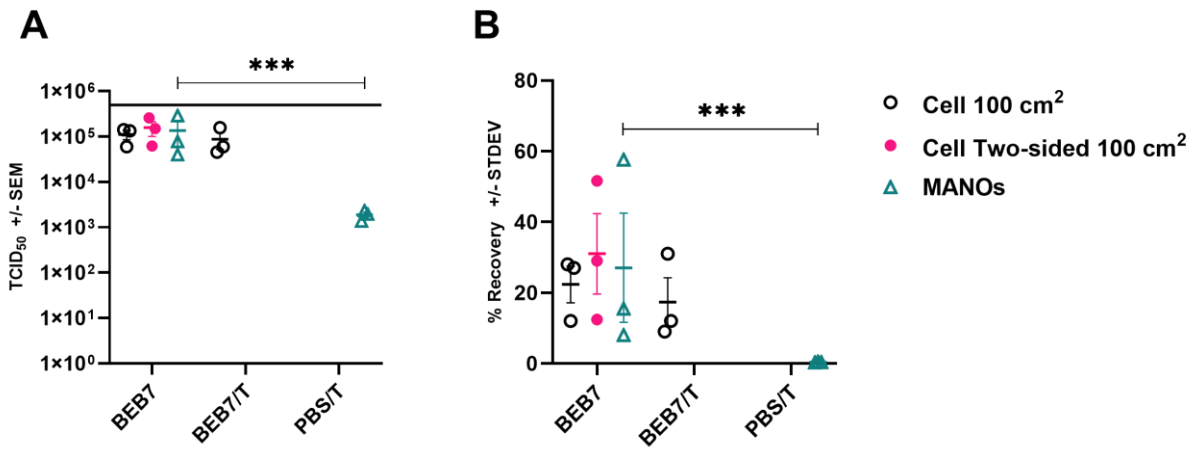

Figure 2.5. SARS-CoV-2 recovery from SS in eluants using samplers.

Total $TCID_{50}$ recovery (A) and percentage of recovery (B.) The horizontal solid line denotes the starting inoculum at 5.01 $\times 10^5$ $TCID_{50}$ for MANOs and cellulose use for optimal sizes. Bars represent the SEM (A) and STDEV (B). The symbol *** denotes the significance levels of a p-value ***: $p \leq 0.001$

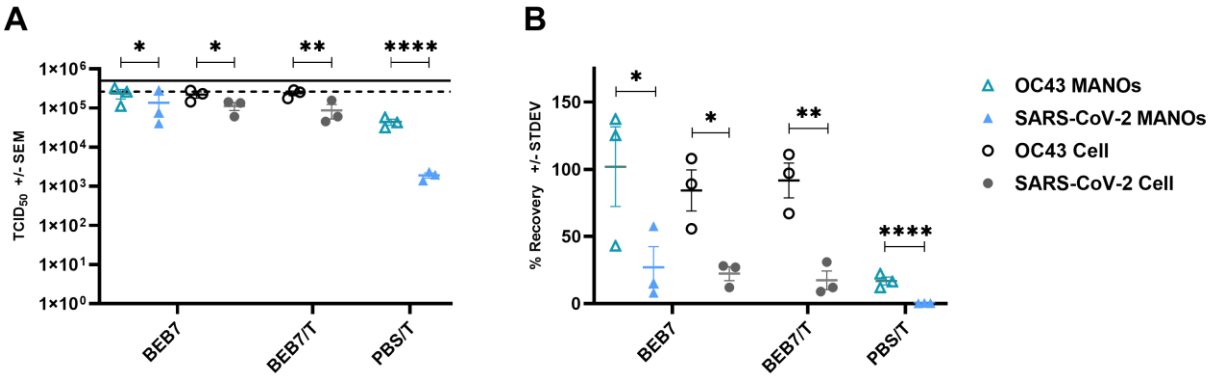

Figure 2.6. Comparison between infectious virus recovery of OC43 and SARS-CoV-2 from SS for MANOs and cellulose at optimal sizes (100 cm^2 and 1,267 cm^2, respectively) in a BSC.

Total $TCID_{50}$ recovery (A) and percentage of recovery (B). The horizontal solid line denotes the starting inoculum of 5.01 $\times 10^5$ $TCID_{50}$ for SARS-CoV-2 experiments, whereas the horizontal dashed line denotes the starting inoculum of 2.61 $\times 10^5$ $TCID_{50}$ for OC43 experiments for MANOs and cellulose for optimal sizes. Bars represent the SEM (A) and STDEV (B). The symbols *, **, and **** denote the significance levels of a p-value where *: $p \leq 0.05$, **: $p \leq 0.01$, ****: $p \leq 0.0001$.

3-3. SARS-CoV-2 Recovery Comparisons in BSL-3 Agriculture Containment

To simulate environmental sampling within M&P facility settings and account for the potential impact of the high air exchange rate within the BSC on infectious SARS-CoV-2 recovery, further experiments were conducted in the BSL-3 Ag containment space. The average air exchange rate for the BSCs used in this study was 100 linear feet per minute, meaning that the air inside the BSC was replaced with new, high-efficiency particulate air (HEPA)-filtered air approximately 50 times per minute [85]. In contrast, the BSL-3 Ag room had the air exchanged with new, HEPA-filtered air at a rate reduced to 6 air changes per hour (ACH). The six ACH aligns with the previous USDA mandate of a minimum of six ACH for meat processing facilities, but processing facilities for ready-to-eat products typically maintain higher rates between 20 to 25 ACH for improved air quality [86]. The high air turnover rate of the BSCs may significantly influence experimental outcomes by rapidly desiccating the virus on surfaces and thereby reducing recovery whereas the BSL-3 Ag room creates a more controlled environment that better reflects real-world conditions and minimizes the potential for rapid desiccation.

Based on the low recovery into PBS/T and no significant observed advantage of BEB7/T over BEB7, these experiments were conducted with BEB7 only. Additionally, to elucidate potential recovery losses from the sponge material, potential virus interaction with the bag material, and residual eluant remaining in the bags, direct inoculation of control sponges and bags was added. Furthermore, a third sponge material, hydrophilic polyurethane, was added based on evidence that this material was a more efficient EM tool in the recovery of bacteria and non-enveloped viruses and in light of our observations regarding the eluant resorption inefficiencies observed for hydrophobic MANOs [74, 87].

Overall, there was significant variability in the recovery of infectious SARS-CoV-2 between sampler types, as well as within MANO formulations, across both optimal and enlarged sizes (**Figure 2.7**). Infectious SARS-CoV-2 recovery from polyurethane was consistently high, with no significant differences observed across the controls and different surface areas (**Figure 2.7 E-F**). For cellulose, a reduction of 84-90% of infectious virus was seen in the control sponge for both optimal and expanded sizes when compared to direct inoculation of the bag ($p = 0.0130$, $p = 0.0186$, and $p = 0.0021$, respectively) (**Figure 2.7 C-D**). Additionally, MANOs showed a 33-42% average reduction in the recovery of infectious virus for both optimal and expanded sizes when compared to the direct inoculation of the bag ($p = 0.0059$ and $p < 0.0001$, respectively). There was also a 46-55% average reduction in recovery with MANOs when compared to the control sponge (= 0.0036 and $p < 0.0001$, respectively) (**Figure 2.7 A-B**).

For the optimal sizes, the only observed difference was an average 30% decrease in virus recovery with MANOs compared to polyurethane ($p = 0.0164$) (**Figure 2.8 A-B**). For the enlarged sizes, cellulose had a 12% greater average percent recovery than MANOs ($p = 0.0091$) (**Figure 2.8 A-B**). Additionally, polyurethane for the optimal size had a 39% greater recovery when compared to MANOs for the expanded area ($p = <0.0001$) (**Figure 2.8 A-B**).

I also explored comparisons between the conservative polyurethane sizes and the optimal/expanded sizes for cellulose and MANOs. There was an average 60-69% increase in virus recovery with polyurethane at 969 cm^2 compared to MANOs at the optimal and expanded sizes (= 0.0005 and $p < 0.0001$, respectively) (**Figure 2.8 A-B**). The other significant finding was a 57% increase in virus recovery using polyurethane at 969 cm^2 compared to cellulose for the expanded size ($p = 0.0151$.) (**Figure 2.8 A-B**). For more detailed information regarding the comparisons between samplers depicted in **Figure 2.8 A-B**, refer to **Table 1**.

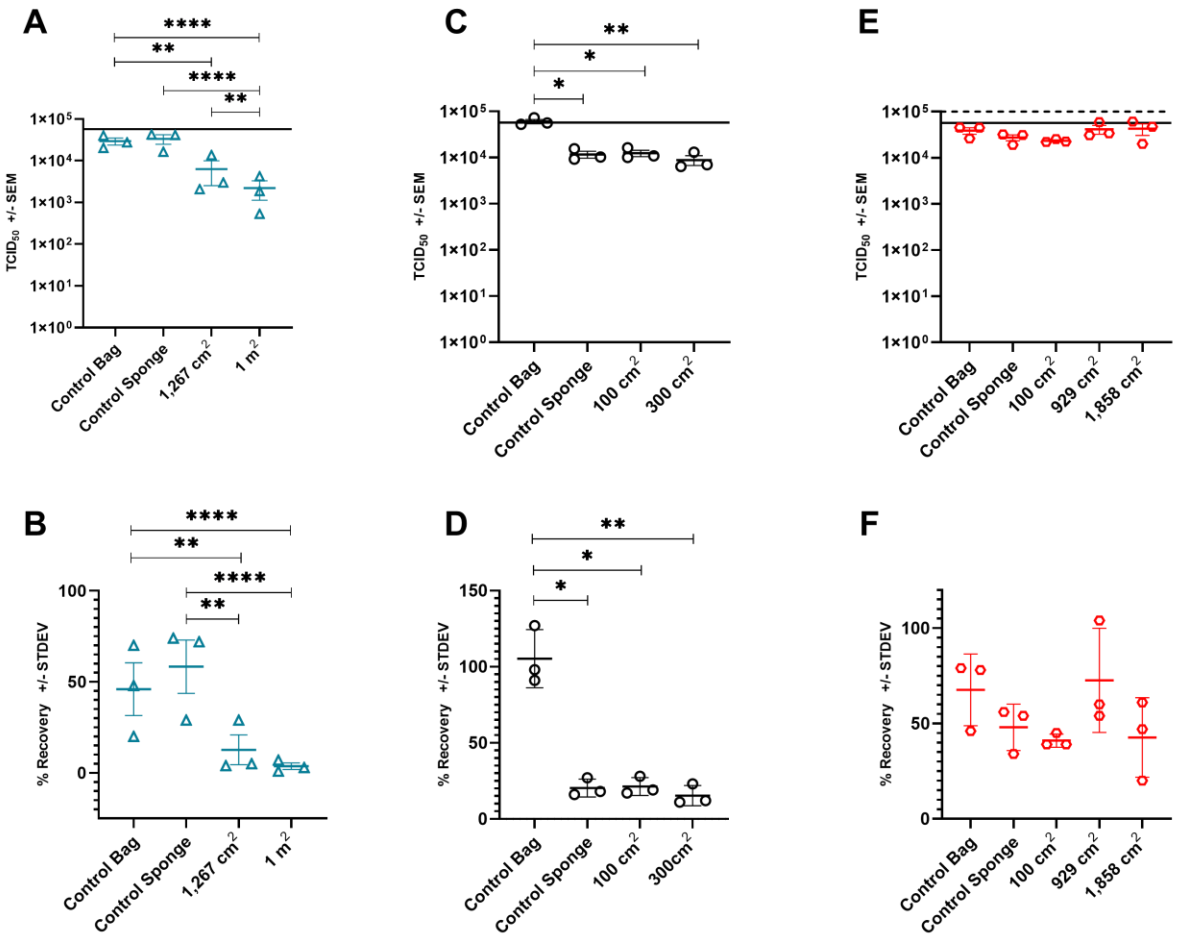

Figure 2.7. Comparison of SARS-CoV-2 recovery from SS in BSL-3 Ag space of sampler controls and their relevant surface areas.

Total $TCID_{50}$ recovery for MANOs, cellulose, and polyurethane (A, C, and E, respectively) and percentage of recovery (B, D, and F, respectively). The horizontal solid line denotes the starting inoculum at 5.72 $\times 10^4$ $TCID_{50}$. The dashed horizontal line denotes the starting inoculum of 1.00 $\times 10^5$ $TCID_{50}$ for the polyurethane 1,858 cm^2 area. Bars represent the SEM (A, C, and E) and STDEV (B, D, and F). The symbols *, **, and **** denote the significance levels of a p-value where *: $p \leq 0.05$, **: $p \leq 0.01$, ****: $p \leq 0.0001$.

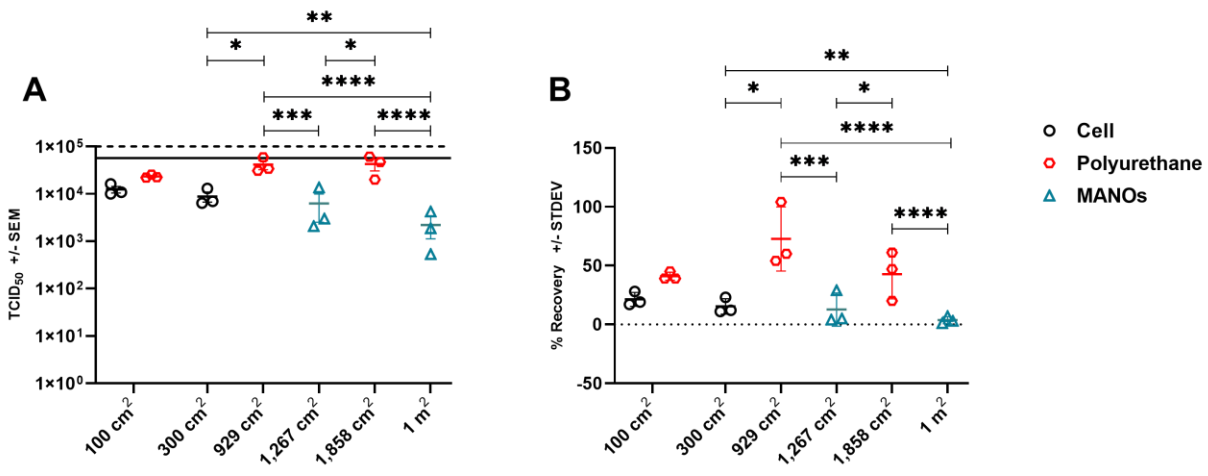

Figure 2.8. Comparison of SARS-CoV-2 recovery from SS in BSL-3 Ag space for different sampler methods.

Total $TCID_{50}$ recovery (A) and percentage of recovery (B). The horizontal solid line denotes the starting inoculum at 5.72 $\times 10^4$ $TCID_{50}$ for all experiments, except polyurethane at the optimal size. The dashed horizontal line denotes the starting inoculum of 1.00 $\times 10^5$ $TCID_{50}$ for the polyurethane at the optimal size. Bars represent the SEM (A) and STDEV (B). The symbols *, **, ***, and **** denote the significance levels of a p-value where *: $p \leq 0.05$, **: $p \leq 0.01$, ***: $p \leq 0.001$, ****: $p \leq 0.0001$

Table 1. SARS-CoV-2 BSL-3 Ag. Sampler Comparisons at Optimal, Conserved, and Enlarged Sizes

Comparison Made	95.00% CI of diff.	Summary	Adjusted p-value
Cellulose 100 cm^2 vs. Polyurethane 100 cm^2	-0.2994 to 0.8718	ns	0.8151
Cellulose 100 cm^2 vs Polyurethane 300 cm^2	-0.9945 to 0.1767	ns	0.2537
Cellulose 100 cm^2 vs. MANO 1,267 cm^2	0.09149 to 1.263	ns	0.3617
Cellulose 300 cm^2 vs. Polyurethane at 929 cm^2	-0.1639 to 1.007	*	0.0151
Cellulose 300 cm^2 vs. Polyurethane at 1,858 cm^2	-0.8350 to 0.3362	ns	0.3214
Cellulose 300 cm^2 vs. MANOs at 1,267 cm^2	-1.300 to -0.1288	ns	0.9127
Cellulose 300 cm^2 vs. MANO's at 1 m^2	-1.512 to -0.3409	**	0.0091
Polyurethane 929 cm^2 vs MANOs 1,267 cm^2	-1.977 to -0.8059	***	0.0005
Polyurethane 929 cm^2 vs MANOs 1 m^2	-1.257 to -0.08543	****	<0.0001
Polyurethane 1,858 cm^2 vs MANOs 1,267 cm^2	-1.722 to -0.5505	*	0.0164
Polyurethane 1,858 cm^2 vs MANOs 1 m^2	-0.1399 to 1.031	****	<0.0001

4. Discussion

Not unsurprisingly, the recovery of infectious coronaviruses from SS surfaces varies with EM sampler, eluant, and sampled area size. Compared to cellulose and MANOs, hydrophilic polyurethane samplers recover a significantly higher percentage of infectious SARS-CoV-2 from larger surface areas when used with BEB7 (**Figure 2.8**). However, the optimal selection of materials for EM in M&P facilities must be tailored to specific needs and existing monitoring programs.

The importance of sponge composition on the recovery percentage of bacteria and non-enveloped viruses from animal carcasses and environmental surfaces was described previously [88-92]. In general, these study results vary in recovery efficacy of bacteria and viruses from several types of sampler material, including cotton, rayon, macrofoam, cellulose, polyester, and polyurethane. Notably, cotton, macrofoam, and polyurethane have been effective in recovering a higher percentage of bacteria [71]. Moreover, it has been observed that, in general, bacteria are more readily released from EM samplers than viruses [57]. Cotton, polyester, polyurethane, and macrofoam materials have all been shown to be effective for the recovery of norovirus, Tulane virus, rotavirus, and M2 bacteriophage [57, 74]. However, the diversity of study designs as regards selected elution buffers, surface sizes and compositions, and microbial detection methods hampers comparison of material efficiency.

The specific pathogen an EM program targets also influences the efficiency of EM sampler types, eluants, and surface area sampled. Our results show a decrease in recovery for the EM samplers when used on their optimal sizes for SARS-CoV-2 compared to OC43 (**Figure 2.6**). Given its extensive study and adaptation through serial passage in cell culture, as well as its increased resistance to disinfectant, OC43 may be more resilient than SARS-CoV-2 [17, 83].

Furthermore, while phosphate-buffered solutions have been shown to be efficient buffers for bacteria, as well as viral genome recovery, PBS/T performed poorly in the recovery of infectious OC43 and SARS-CoV-2 compared to BEB7 (**Figures 2.4-2.6**) [93, 94].

I used a neutral buffer (BEB7) to elute virus particles from the sponges. At neutral pH, the SARS-CoV-2 virion has a net negative charge, meaning that electrostatic forces can significantly influence its interaction with the sponge materials [95]. The sponge material used in this study likely carries a charge that can vary depending on its material properties. Moreover, due to the triboelectric effect wherein certain materials become electrically charged post frictional contact, it is possible that when the sponges interact with the SS surface, they acquire a charge that influences their interaction with the negatively charged virions [96]. This electrostatic interaction could either lead to stronger adherence or repulsion of the virions, potentially hindering or facilitating elution. Since the specific charge that occurs on the sponge material is unknown, a more basic buffer solutions as well as specific charge measurement may be worth exploring. Electrostatic forces are known to play a significant role in the recovery of enteric viruses from wastewater, where electropositive or electronegative filters are used to collect the virus [97]. For these techniques, the U.S. Environmental Protection Agency recommends using a 1.5% beef extract with 0.05 M glycine at pH 9.5 as an elution buffer, which has been effective in reducing electrostatic attractions and improving recovery rates [98]. Therefore, a buffer with a higher pH could similarly neutralize the virions, reducing attraction and enhancing the release and recovery of SARS-CoV-2 during the elution process.

I also observed significant differences in the recovery of SARS-CoV-2 when using MANOs compared to cellulose and polyurethane sponges. The hydrophobic nature of the MANOs could be responsible for the decreased recovery of infectious viruses. During use, I

observed that a large amount of eluant (approximately 60-75%) was left on the surface after sampling. This loss of eluant may have led to virus desiccation and degradation on the sponge surface. Additionally, since little eluant (approximately 5 – 8 ml) remained to elute any virus from the sampler during processing, it is also likely that virus remained on the surface in the buffer that the MANO was unable to soak up. Hydrophilic materials, on the other hand, tend to retain eluant, facilitating uptake into the sponge material and this may prevent the desiccation and loss of infectious virus. The contrast between hydrophobic and hydrophilic materials' infectious virus recovery capability became even more apparent when using polyurethane compared to MANOs, especially for larger surface areas. In such scenarios, the increased area available for wiping presented more opportunities for eluant loss, further diminishing the efficacy of MANO virus recovery.

Several constraints are apparent in the current research. First, while I attempted to recreate aspects of the M&P settings within the BSL-3 Ag space, this study was still conducted in a laboratory setting. Only SS surfaces, the most abundant in these facilities, were tested; however, other surface types such as plastic, glass, and rubber are also present and may interact differently with the virus. While air exchange rates within the BSL-3 Ag space were reduced to six per hour and temperature and humidity were held constant within a range of 61.2°F to 70.7°F and 52.7% to 78.8%, respectively., these conditions fail to fully capture the variability found in M&P environments, particularly regarding climate fluctuations and the constant movement of workers and machinery. For example, meat cutting rooms typically maintain temperatures between 10°C and 12°C with relative humidity levels of 45% to 60%, while coolers are kept at much lower temperatures, around 0°C to 4°C, with higher humidity levels of 85% to 95% to prevent drying and weight loss [28, 99]. Given these constraints, the study's findings may have

limited generalizability to real-world M&P environments, where a broader range of surface types and fluctuating climatic conditions can significantly influence virus persistence and recovery.

I also used a high virus inoculation level, concentrating it within the defined surface areas—an approach that likely does not accurately reflect the natural occurrence and distribution of respiratory viruses in real-world environments. Research on SARS-CoV-2 has shown that the viral load in respiratory droplets varies widely, with many particles containing little to no virions, and that viral distribution in indoor settings is often patchy—affected by factors like airflow, surface type, and human activity—resulting in significant variation in contamination levels [100, 101]. The inconsistent inoculation levels of the virus used in each experiment could also impact the study's findings by influencing the efficiency of virus recovery. Higher concentrations might lead to more robust identification compared to lower concentrations of viral contamination. This variation in inoculation levels could also contribute to increased interstudy variability, making it challenging to directly compare results across different experiments and leading to inconsistent conclusions about the effectiveness of recovery methods. Moreover, this study is limited by its reliance on small sample sizes and its exclusive focus on recovery using samplers on manufacturer-recommended surface areas, which vary significantly. There is also inherent variability in the $TCID_{50}$ assay used to quantify infectious virus, and when coupled with a small sample size, it can impact the precision and reliability of the result. Finally, the experimental design overlooks other critical factors, such as opportunities for virus desiccation and instances where the virus may become trapped within the material.

Investigators should consider testing the recovery capabilities of EM samplers and eluants across similar surface area sizes to determine their individual efficiency more accurately. Furthermore, percent recovery for each sampler, eluant, and area combination should be assessed

at serial decreases of virus titer to determine their limit of detection. Also, RT-qPCR could be employed to determine whether the lost infectious virus was inactivated during recovery or lost on the surface or sampler. Given the nature of respiratory viruses being transmitted via respiratory droplets and aerosols, it would also be important to recreate transmission in the manner of a cough, sneeze, etc., to contaminate the surface as opposed to direct inoculation. This way the impact of droplet and/or aerosol deposition onto surfaces and their subsequent infectious viral load could be accounted for as a component in the accurate assessment of sampler efficiency for EM program development.

5. Conclusion

Material selection is critically important to the optimization of EM performance as regards infectious enveloped virus recovery in M&P environments. Although I found that polyurethane generally outperformed its counterparts in most comparisons, there were multiple significant differences found in this study related to eluant and surface area selection as well. Future research should investigate the mechanisms behind these described differences to determine how to improve virus recoverability. Other potential lines of investigation include exploring the influence of extrinsic factors such as climate, cleaning and sanitation procedures, airflow, and sample storage and processing on the recovery of enveloped viruses using various EM methods. The information gathered in such research would assist with future endeavors in EM, enhancing our grasp of viral transmission within M&P establishments and aiding in development of impactful preventive measures. Irrespective, my effort underscores the need for careful consideration when selecting appropriate materials for specific EM program goals.

Chapter 3 - Conclusion

The COVID-19 pandemic heavily impacted many global sectors, causing severe socio-economic and public health impacts. The M&P industry was disproportionately affected because of several intrinsic and extrinsic factors, leading to disruptions in the food supply chains, workforce shortages, and significant alterations in working conditions. M&P workplace settings often involve close contact between workers, enclosed spaces, and shared equipment, all of which heightened the risk of virus transmission. The situation was further exacerbated by challenges in swiftly implementing and adapting to new safety guidelines and preventive measures. The need for continued, uninterrupted plant operations for a demanding consumer market amidst a global health crisis placed additional pressure on facilities. This resulted in a critical examination of workplace safety protocols, prompting calls for innovative and effective strategies to mitigate the risk of SARS-CoV-2 transmission. The pandemic underscored the importance of resilient and adaptable systems within the M&P sector, driving a reevaluation of practices and spurring advancements in EM and infection control to safeguard the health and well-being of the workforce.

As such, the culmination of this research marks a significant stride forward in our understanding of EM practices tailored for the recovery of infectious SARS-CoV-2 virus particles. The findings help provide actionable insights to improve prevention and control measures in M&P settings. The systematic evaluation of the efficacy of various EM materials has helped illuminate pathways to optimize virus detection and surface decontamination strategies, integral components of a robust public health response to respiratory pandemics.

Importantly, the comparative analysis of cellulose, hydrophilic polyurethane, and MANO sponges revealed disparities in material performance for different surface sizes and using

different eluants, underscoring the importance of material selection in EM practices. The superior performance of polyurethane sponge on larger surface areas emerged as a key finding, positioning this material as a promising option for enhanced infectious SARS-CoV-2 recovery from stainless-steel surfaces. These results serve as a valuable resource for stakeholders involved in EM, workplace safety, and infection control.

The observed variability in material performance across different EM comparisons and OC43 compared to SARS-CoV-2 underscores the complexity of EM for infectious viruses and the need for continued research and innovation. As we reflect on this study's findings, it is evident that integrating these insights into practice requires a collaborative effort, bridging the gaps between academia, industry, and public health authorities.

In conclusion, this thesis provides a comprehensive evaluation of EM materials for the recovery of infectious SARS-CoV-2 virus particles, addressing a critical knowledge gap and laying the groundwork for future advancements in this domain.

References

1. Zhu, N., et al., *A Novel Coronavirus from Patients with Pneumonia in China, 2019.* N Engl J Med, 2020. **382**(8): p. 727-733.
2. Zhou, H., et al., *A Review of SARS-CoV2: Compared With SARS-CoV and MERS-CoV.* Front Med (Lausanne), 2021. **8**: p. 628370.
3. Centers for Disease, C. and Prevention, *Revised U.S. surveillance case definition for severe acute respiratory syndrome (SARS) and update on SARS cases--United States and worldwide, December 2003.* MMWR Morb Mortal Wkly Rep, 2003. **52**(49): p. 1202-6.
4. Azhar, E.I., et al., *Evidence for camel-to-human transmission of MERS coronavirus.* N Engl J Med, 2014. **370**(26): p. 2499-505.
5. Haagmans, B.L., et al., *Middle East respiratory syndrome coronavirus in dromedary camels: an outbreak investigation.* Lancet Infect Dis, 2014. **14**(2): p. 140-5.
6. World Health Organization, W. *Middle East respiratory syndrome coronavirus (MERS-CoV)*. 2022 [cited 2023 November 14]; Available from: https://www.who.int/news-room/fact-sheets/detail/middle-east-respiratory-syndrome-coronavirus-(mers-cov).
7. Byambasuren, O., et al., *Estimating the extent of asymptomatic COVID-19 and its potential for community transmission: Systematic review and meta-analysis.* J Assoc Med Microbiol Infect Dis Can, 2020. **5**(4): p. 223-234.
8. Verma, B.K., et al., *Global lockdown: An effective safeguard in responding to the threat of COVID-19.* J Eval Clin Pract, 2020. **26**(6): p. 1592-1598.
9. *WHO COVID-19 Dashboard Geneva*. 2023, World Health Organization.
10. Hassan, I., et al., *Lessons from COVID-19 must be learned before the next outbreak.* Nat Med, 2023. **29**(9): p. 2171-2173.
11. Jackson, C.B., et al., *Mechanisms of SARS-CoV-2 entry into cells.* Nat Rev Mol Cell Biol, 2022. **23**(1): p. 3-20.
12. Cubuk, J., et al., *The SARS-CoV-2 nucleocapsid protein is dynamic, disordered, and phase separates with RNA.* Nat Commun, 2021. **12**(1): p. 1936.
13. Rahman, M.S., et al., *Mutational insights into the envelope protein of SARS-CoV-2.* Gene Rep, 2021. **22**: p. 100997.
14. Zhang, Z., et al., *Structure of SARS-CoV-2 membrane protein essential for virus assembly.* Nat Commun, 2022. **13**(1): p. 4399.
15. Lu, R., et al., *Genomic characterisation and epidemiology of 2019 novel coronavirus: implications for virus origins and receptor binding.* Lancet, 2020. **395**(10224): p. 565-574.
16. Kutter, J.S., et al., *Transmission routes of respiratory viruses among humans.* Curr Opin Virol, 2018. **28**: p. 142-151.
17. Wood, A. and D. Payne, *The action of three antiseptics/disinfectants against enveloped and non-enveloped viruses.* J Hosp Infect, 1998. **38**(4): p. 283-95.
18. Greenberg, S.B., *Update on Human Rhinovirus and Coronavirus Infections.* Semin Respir Crit Care Med, 2016. **37**(4): p. 555-71.
19. Tellier, R., *COVID-19: the case for aerosol transmission.* Interface Focus, 2022. **12**(2): p. 20210072.
20. Zhao, X., et al., *Airborne transmission of COVID-19 virus in enclosed spaces: An overview of research methods.* Indoor Air, 2022. **32**(6): p. e13056.

21. Onakpoya, I.J., et al., *SARS-CoV-2 and the role of fomite transmission: a systematic review.* F1000Res, 2021. **10**: p. 233.
22. Gunther, T., et al., *SARS-CoV-2 outbreak investigation in a German meat processing plant.* EMBO Mol Med, 2020. **12**(12): p. e13296.
23. Morris, D.H., et al., *Mechanistic theory predicts the effects of temperature and humidity on inactivation of SARS-CoV-2 and other enveloped viruses.* eLife, 2021. **10**: p. e65902.
24. Thippareddi, H., et al., *Coronaviruses - Potential human threat from foodborne transmission?* Lebensm Wiss Technol, 2020. **134**: p. 110147.
25. Economic Research Service, U. *Statistics & Information*. [cited 2023; Available from: https://www.ers.usda.gov/topics/animal-products/cattle-beef/statistics-information/.
26. Statistics, U.S.B.o.L. *Occupational Employment and Wage Statistics*. 2022 [cited 2023; Available from: https://www.bls.gov/oes/current/oes513023.htm.
27. Ijaz, M., et al., *Meat Production and Supply Chain Under COVID-19 Scenario: Current Trends and Future Prospects.* Front Vet Sci, 2021. **8**: p. 660736.
28. Taylor, C.A., C. Boulos, and D. Almond, *Livestock plants and COVID-19 transmission.* Proc Natl Acad Sci U S A, 2020. **117**(50): p. 31706-31715.
29. Dyal JW, G.M., Broadwater K, et al., *COVID-19 Among Workers in Meat and Poultry Processing Facilities — 19 States.* MMWR Morb Mortal Wkly Rep, 2020.
30. (CDC), C.f.D.C.a.P. *Symptoms of COVID-19*. [cited 2023 12/01]; Available from: https://www.cdc.gov/coronavirus/2019-ncov/symptoms-testing/symptoms.html.
31. (NIH), N.I.o.H. *Clinical Spectrum of SARS-CoV-2 Infection*. 2023 [cited 2023 12/01]; Available from: https://www.covid19treatmentguidelines.nih.gov/overview/clinical-spectrum/.
32. Becerra-Munoz, V.M., et al., *Clinical profile and predictors of in-hospital mortality among older patients hospitalised for COVID-19.* Age Ageing, 2021. **50**(2): p. 326-334.
33. Schultz, M.J., P.J. van Oosten, and L. Hol, *Mortality among elderly patients with COVID-19 ARDS-age still does matter.* Pulmonology, 2023. **29**(5): p. 353-355.
34. Chen, C., et al., *Global Prevalence of Post-Coronavirus Disease 2019 (COVID-19) Condition or Long COVID: A Meta-Analysis and Systematic Review.* J Infect Dis, 2022. **226**(9): p. 1593-1607.
35. Raveendran, A.V., R. Jayadevan, and S. Sashidharan, *Long COVID: An overview.* Diabetes Metab Syndr, 2021. **15**(3): p. 869-875.
36. Kim, Y., et al., *Long COVID prevalence and impact on quality of life 2 years after acute COVID-19.* Sci Rep, 2023. **13**(1): p. 11207.
37. L, O.M., et al., *Impact of Long COVID on health and quality of life.* HRB Open Res, 2022. **5**: p. 31.
38. (SAMHSA), S.A.a.M.H.S.A., *Overview of the Impacts of Long Covid on Behavioral Health*. 2023, U.S. Department of Health and Human Services (HHS): Rockville, MD.
39. Malesevic, S., et al., *Impaired health-related quality of life in long-COVID syndrome after mild to moderate COVID-19.* Sci Rep, 2023. **13**(1): p. 7717.
40. Krumel, T., Goodrich, Corey, *COVID-19 Working Paper: Meatpacking Working Conditions and the Spread of COVID-19.* USDA Economic Research Service COVID-19 Working Paper series, 2021. **AP-092**.
41. Russell, C.D., N.I. Lone, and J.K. Baillie, *Comorbidities, multimorbidity and COVID-19.* Nat Med, 2023. **29**(2): p. 334-343.

42. Hashem, N.M., A. Gonzalez-Bulnes, and A.J. Rodriguez-Morales, *Animal Welfare and Livestock Supply Chain Sustainability Under the COVID-19 Outbreak: An Overview.* Front Vet Sci, 2020. **7**: p. 582528.
43. Martini, M., et al., *The Spanish Influenza Pandemic: a lesson from history 100 years after 1918.* J Prev Med Hyg, 2019. **60**(1): p. E64-E67.
44. Rockman, S., K. Laurie, and I. Barr, *Pandemic Influenza Vaccines: What did We Learn from the 2009 Pandemic and are We Better Prepared Now?* Vaccines (Basel), 2020. **8**(2).
45. Wang, H., et al., *The genetic sequence, origin, and diagnosis of SARS-CoV-2.* Eur J Clin Microbiol Infect Dis, 2020. **39**(9): p. 1629-1635.
46. CDC, *Meat and poultry processing workers and employers : interim guidance from CDC and the Occupational Safety and Health Administration (OSHA),* C.f.D.C.a.P.U.S.U.S.O.S.a.H.A.N.C.f.I.a.R.D.U.S.D. of, Editor. 2020, CDC.
47. Herstein, J.J., et al., *Characteristics of SARS-CoV-2 Transmission among Meat Processing Workers in Nebraska, USA, and Effectiveness of Risk Mitigation Measures.* Emerg Infect Dis, 2021. **27**(4): p. 1032-1038.
48. Fabreau, G.E., et al., *Vaccines alone will not prevent COVID-19 outbreaks among migrant workers-the example of meat processing plants.* Clin Microbiol Infect, 2022. **28**(6): p. 773-778.
49. Tang, J.W., et al., *An exploration of the political, social, economic and cultural factors affecting how different global regions initially reacted to the COVID-19 pandemic.* Interface Focus, 2022. **12**(2): p. 20210079.
50. Wilkinson A, M.H., Scoones I, Schmidt-Sane M, Leach M, Taylor P, Ripoll S, Khan Mohmand S, Abbas S, Hrynick T., *Pandemic Preparedness for the Real World: Why We Must Invest in Equitable, Ethical and Effective Approaches to Help Prepare for the Next Pandemic.* Institute of Developmental Studies, 2023.
51. Raphael, S. and D. Schneider, *Introduction: The Socioeconomic Impacts of COVID-19.* RSF: The Russell Sage Foundation Journal of the Social Sciences, 2023. **9**(3): p. 1-30.
52. Vigo, D., et al., *Mental Health of Communities during the COVID-19 Pandemic.* Can J Psychiatry, 2020. **65**(10): p. 681-687.
53. Witteveen, A.B., et al., *COVID-19 and common mental health symptoms in the early phase of the pandemic: An umbrella review of the evidence.* PLOS Medicine, 2023. **20**(4): p. e1004206.
54. Unicef, *The state of the global education crisis: a path to recovery: a joint UNESCO, UNICEF and WORLD BANK report*. 2021: Paris: UNESCO, cop. 2021.
55. Rydland, H.T., et al., *The radically unequal distribution of Covid-19 vaccinations: a predictable yet avoidable symptom of the fundamental causes of inequality.* Humanities and Social Sciences Communications, 2022. **9**(1): p. 61.
56. De Oliveira Mota, J., Boué, G., Prévost, H., Maillet, A., Jaffres, E., Maignien, T., Arnich, N., Sanaa, M., & Federighi, M., *Environmental monitoring program to support food microbiological safety and quality in food industries: A scoping review of the research and guidelines.* Food Control, 2021. **130**.
57. Jones, S.L. and K.E. Gibson, *Factors impacting microbial release from environmental monitoring tools.* Int J Food Microbiol, 2021. **347**: p. 109198.
58. Waltenburg, M.A., et al., *Update: COVID-19 Among Workers in Meat and Poultry Processing Facilities - United States, April-May 2020.* MMWR Morb Mortal Wkly Rep, 2020. **69**(27): p. 887-892.

59. Kate Vaiknoras, W.H., Samantha L. Padilla, Adriana Valcu-Lisman, and Grace Grossen, *COVID-19 Working Paper: COVID-19 and the U.S. Meat and Poultry Supply Chains*, in *COVID-19 Working Paper*. 2022, USDA Economic Research Service.
60. Ijaz, M., et al., *Meat production and supply chain under COVID-19 scenario: Current trends and future prospects.* Frontiers in Veterinary Science, 2021. **8**: p. 660736.
61. Council, N.P.P. *Hog Farmers Face COVID-19 Financial Crisis*. 2020 [cited 2024 August 11]; Available from: https://nppc.org/press-releases/hog-farmers-face-covid-19-financial-crisis/.
62. Fears, A.C., et al., *Persistence of Severe Acute Respiratory Syndrome Coronavirus 2 in Aerosol Suspensions.* Emerg Infect Dis, 2020. **26**(9): p. 2168-71.
63. Marques, M. and J.L. Domingo, *Contamination of inert surfaces by SARS-CoV-2: Persistence, stability and infectivity. A review.* Environ Res, 2021. **193**: p. 110559.
64. Butot, S., et al., *Data on Transfer of Human Coronavirus SARS-CoV-2 from Foods and Packaging Materials to Gloves Indicate That Fomite Transmission Is of Minor Importance.* Appl Environ Microbiol, 2022. **88**(7): p. e0233821.
65. Mondelli, M.U., et al., *Low risk of SARS-CoV-2 transmission by fomites in real-life conditions.* Lancet Infect Dis, 2021. **21**(5): p. e112.
66. Beno, S.M., et al., *Development and Validation of Pathogen Environmental Monitoring Programs for Small Cheese Processing Facilities.* J Food Prot, 2016. **79**(12): p. 2095-2106.
67. Bourdichon, F., et al., *Processing environment monitoring in low moisture food production facilities: Are we looking for the right microorganisms?* Int J Food Microbiol, 2021. **356**: p. 109351.
68. Kovacevic, J., et al., *Evaluation of environmental sampling methods and rapid detection assays for recovery and identification of Listeria spp. from meat processing facilities.* J Food Prot, 2009. **72**(4): p. 696-701.
69. Zoellner, C., et al., *Design Elements of Listeria Environmental Monitoring Programs in Food Processing Facilities: A Scoping Review of Research and Guidance Materials.* Compr Rev Food Sci Food Saf, 2018. **17**(5): p. 1156-1171.
70. 3M, C.U., *Environmental monitoring handbook for the food and beverage industries.* 3M, USA, 2019.
71. Jones, S.L., et al., *Swabbing the surface: critical factors in environmental monitoring and a path towards standardization and improvement.* Crit Rev Food Sci Nutr, 2020. **60**(2): p. 225-243.
72. *FDA Food Safety Modernization Act*, in *124*. 2011, U.S. Government Publishing Office: United States. p. 3885 - 3973.
73. FSIS, U. *FSIS Guidelines*. [cited 2023 11/30]; Available from: https://www.fsis.usda.gov/policy/fsis-guidelines.
74. Jones, S.L. and K.E. Gibson, *Characterization of Polyurethane Foam Environmental Monitoring Tools for the Recovery and Release of Viruses.* Food Environ Virol, 2020. **12**(2): p. 158-166.
75. Jones, T.H., V. Muehlhauser, and G. Croken, *Development of an optimized method for the recovery of infectious F-RNA coliphage MS2 from meat.* J Virol Methods, 2012. **185**(1): p. 69-73.
76. Lee, C., et al., *Comparison of Swab Sampling Methods for Norovirus Recovery on Surfaces.* Food Environ Virol, 2018. **10**(4): p. 378-385.

77. Miyazaki, H., et al., *Methods for virus recovery from environmental surfaces to monitor infectious viral contamination.* Environ Int, 2023. **180**: p. 108199.
78. Mo, J., et al., *Optimizing sample collection methods for detection of respiratory viruses in poultry housing environments.* Transbound Emerg Dis, 2022. **69**(5): p. e2111-e2121.
79. Tung-Thompson, G., et al., *Evaluation of a Surface Sampling Method for Recovery of Human Noroviruses Prior to Detection Using Reverse Transcription Quantitative PCR.* J Food Prot, 2017. **80**(2): p. 231-236.
80. Cevik, M., et al., *SARS-CoV-2, SARS-CoV, and MERS-CoV viral load dynamics, duration of viral shedding, and infectiousness: a systematic review and meta-analysis.* Lancet Microbe, 2021. **2**(1): p. e13-e22.
81. Abrahao, J.S., et al., *Detection of SARS-CoV-2 RNA on public surfaces in a densely populated urban area of Brazil: A potential tool for monitoring the circulation of infected patients.* Sci Total Environ, 2021. **766**: p. 142645.
82. Dohla, M., et al., *SARS-CoV-2 in Environmental Samples of Quarantined Households.* Viruses, 2022. **14**(5).
83. Schirtzinger, E.E., Y. Kim, and A.S. Davis, *Improving human coronavirus OC43 (HCoV-OC43) research comparability in studies using HCoV-OC43 as a surrogate for SARS-CoV-2.* Journal of Virological Methods, 2022. **299**: p. 114317.
84. L.J. REED, H.M., *A SIMPLE METHOD OF ESTIMATING FIFTY PER CENT ENDPOINTS.* American Journal of Epidemiology, 1938. **27**(3): p. 493-497.
85. *Nuaire Biological Safety Cabinets Catalog*. NuAire, Inc.
86. Graham, D., *In-plant Air Handling and Food Safety: There Is a Connection*, in *Food Safety Magazine*. 2011.
87. Keeratipibul, S.L., Thamolwan ; Pornruangsarp, Orapin ; Chaturongkasumrit, Yuphakhun ; Takahashi, Hajime ; Techaruvichit, Punnida, *Effect of swabbing techniques on the efficiency of bacterial recovery from food contact surfaces.* Food control, 2017. **77**: p. 139-144.
88. Jansson, L., et al., *Impact of swab material on microbial surface sampling.* J Microbiol Methods, 2020. **176**: p. 106006.
89. Martinez, B., et al., *Microbiological sampling of carcasses by excision or swabbing with three types of sponge or gauze.* J Food Prot, 2010. **73**(1): p. 81-7.
90. Park, G.W., et al., *Evaluation of a New Environmental Sampling Protocol for Detection of Human Norovirus on Inanimate Surfaces.* Appl Environ Microbiol, 2015. **81**(17): p. 5987-92.
91. Pearce, R.A. and D.J. Bolton, *Excision vs sponge swabbing - a comparison of methods for the microbiological sampling of beef, pork and lamb carcasses.* J Appl Microbiol, 2005. **98**(4): p. 896-900.
92. Rose, L., et al., *Swab materials and Bacillus anthracis spore recovery from nonporous surfaces.* Emerg Infect Dis, 2004. **10**(6): p. 1023-9.
93. Kirkland, P.D., Frost, M.J., *The impact of viral transport media on PCR assay results for the detection of nucleic acid from SARS-CoV-2.* Pathology, 2020. **52**(7): p. 811-814.
94. Perchetti, G.A., et al., *Stability of SARS-CoV-2 in Phosphate-Buffered Saline for Molecular Detection.* J Clin Microbiol, 2020. **58**(8).
95. Cotten, M. and M.V.T. Phan, *Evolution of increased positive charge on the SARS-CoV-2 spike protein may be adaptation to human transmission.* iScience, 2023. **26**(3): p. 106230.

96. Zou, H., et al., *Quantifying the triboelectric series.* Nature Communications, 2019. **10**(1): p. 1427.
97. Lee, H., et al., *Evaluation of electropositive filtration for recovering norovirus in water.* Journal of water and health, 2011. **9**(1): p. 27-36.
98. Williams, F., R. Stetler, and R. Safferman, *USEPA manual of methods for virology.* Environmental Protection Agency, 2001. **600**: p. 4-84.
99. U.S. Department of Agriculture, F.S.a.I.S.F., *Pathogen Reduction; Hazard Analysis and Critical Control Point (HACCP) Systems; Final Rule*. 1996, Federal Register: Code of Federal Regulation.
100. Dhand, R. and J. Li, *Coughs and Sneezes: Their Role in Transmission of Respiratory Viral Infections, Including SARS-CoV-2.* Am J Respir Crit Care Med, 2020. **202**(5): p. 651-659.
101. Stadnytskyi, V., P. Anfinrud, and A. Bax, *Breathing, speaking, coughing or sneezing: What drives transmission of SARS-CoV-2?* J Intern Med, 2021. **290**(5): p. 1010-1027.